Chemical Engineering Journal 148 (2009) 201–206

Contents lists available at ScienceDirect

Chemical Engineering Journal

journal homepage: www.elsevier.com/locate/cej

Preparation and properties of sulfonated carbon–silica composites from sucrose dispersed on MCM-48

Ya Liu [a], Jun Chen [a], Jianfeng Yao [a], Yong Lu [b], Lixiong Zhang [a,*], Xiaoqin Liu [a]

[a] State Key Laboratory of Material-Oriented Chemical Engineering, College of Chemistry and Chemical Engineering, Nanjing University of Technology, 5 Xin Mofan Road, Nanjing 210009, PR China
[b] Shanghai Key Laboratory of Green Chemistry and Chemical Processes, Department of Chemistry, East China Normal University, Shanghai 200062, PR China

ARTICLE INFO

Article history:
Received 24 September 2008
Received in revised form 3 January 2009
Accepted 7 January 2009

Keywords:
Sulfonation
Carbon–silica composite
MCM-48
Sucrose

ABSTRACT

Sulfonated carbon–silica composites with surface areas of over 600 m^2/g and pore sizes of 1.5–2.2 nm were prepared by incompletely carbonizing sucrose dispersed on MCM-48 and sulfonating the obtained carbon/MCM-48 composites. The samples were characterized by X-ray diffraction, scanning electron microscopy, transmission electron microscopy, thermogravimetric analysis, N_2 adsorption, energy dispersive X-ray analysis, and X-ray photoelectron spectroscopy. The catalytic activities of these composites were studied in the esterification of acetic acid with n-butyl alcohol. The pore sizes and catalytic activities of the sulfonated carbon–silica composites were adjustable by changing the amount of sucrose loadings, and the composites exhibited enhanced hydrothermal stability and amphiphilic property. When the sucrose loading was close to the monolayer dispersion capacity of sucrose on MCM-48 (1.1 g sucrose/g MCM-48), the resulting sulfonated carbon–silica composites exhibited surface areas of 700–724 m^2/g and n-butyl acetate yields of 90.4–98.7% in the esterification of acetic acid with n-butyl alcohol. They also showed obvious catalytic activities in the esterification of long-chain fatty acids with ethanol. The expensive MCM-48 could be easily recycled by simply calcining the sulfonated carbon–silica composites in air.

1. Introduction

Liquid acids, such as H_2SO_4, HF and H_3PO_4, are widely used as catalysts in industrial catalytic processes. Because of their toxic and corrosive properties, there have been increasing demands to replace them with recyclable solid acids [1], which are environmentally friendly and can be easily separated. One of the very attracting techniques to develop solid acids is to integrate acidic functional groups (e.g. $–SO_3H$) into ordered mesoporous silicas (OMSs), which can be produced by direct- [2,3] or post- [4,5] synthesis methods. The direct synthesis method involves a one-step synthetic strategy based on co-condensation of tetraethoxysilane (TEOS) and 3-mercatopropyl trimethoxysilane in the presence of block copolymers template; while the post-synthesis method involves the organization of a thiol and sulfonate ester functional groups onto the mesoporous silica [4], and followed by oxidation of –SH to $–SO_3H$ group with H_2O_2 [2,3]. However, the resulting acidic OMSs have relatively low $–SO_3H$ density and low hydrothermal stability in boiling water. Sulfonation of incompletely carbonized natural organic products, such as naphthalene [6], sucrose [7] and starch [8], can result in the formation of stable acid carbons with a high density of active sites in the range of 0.37–1.34 mmol/g [9]. But these carbons are non-ordered [8] and nonporous [9] and exhibited low BET surface areas (2 m^2/g), which limits their further applications. In order to prepare acidic carbons with ordered structure and high surface areas, ordered mesoporous carbons (OMCs) are functionalized with $–SO_3H$ functional group by different methods, such as sulfonation of OMCs through contacting CMK-3 with the vapor from fuming sulfuric acid in a closed autoclave [10] or covalent attachment on the surface of CMK-5 [11]. However, the preparation of OMCs usually sacrifices expensive mesoporous silica templates, resulting in waste of resources and energy.Recently, mesoporous carbon/silica composite materials prepared by coating carbon on the inner surface of OMSs have attracted much attention. Ribeiro Carrott et al. [12] modified the surface of MCM-41 with carbon via chemical vapor deposition of benzene. Kim et al. [13] and Zhu et al. [14] graphitized in situ as-made mesoporous MSU and SBA-15 containing non-ionic surfactant micelles to form carbon film on the internal surfaces of OMSs, respectively. The carbon-coated SBA-15 was also prepared by grafting 2,3-dihydroxynaphthalene (DN) through a dehydration reaction between the surface silanol groups in SBA-15 and the hydroxyl groups of the DN molecules and then carbonizing DN in the SBA-15 pores [15]. These materials inherited

* Corresponding author. Tel.: +86 25 83172265; fax: +86 25 83172261.
E-mail address: lixiongzhang@yahoo.com (L. Zhang).

1385-8947/$ – see front matter © 2009 Elsevier B.V. All rights reserved.
doi:10.1016/j.cej.2009.01.010

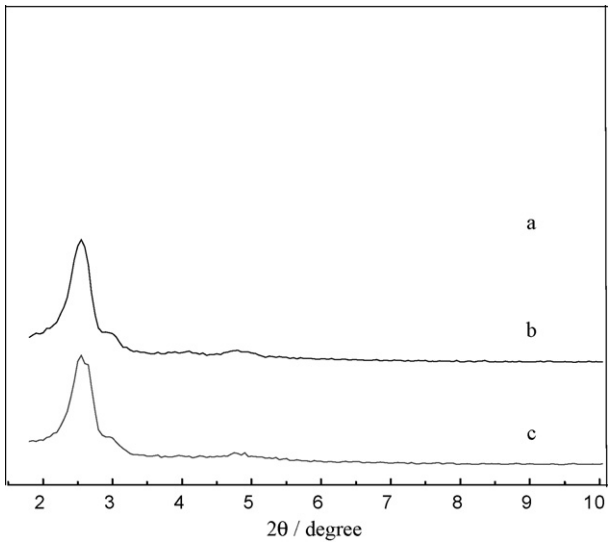

Fig. 1. Small-angle XRD patterns of MCM-48 (a), C-MC-1.2 (b) and MC-1.2 (c).

pore structure of OMSs and exhibited surface chemistry analogous to carbon, such as remarkable hydrophobicity and high electrical conductivity [13–15]. Additionally, the hydrothermal stability of OMSs could be improved after introducing carbon [12]. More work has been carried out to functionalize this kind of material as solid acid catalysts.

Inspired by the preparation and unique properties of mesoporous carbon/silica composite [6–9], we aim to cover incompletely carbonized natural organic products on the internal surface of OMSs and then introduce $-SO_3H$ via sulfonation so as to prepare a novel solid acid with the pore structure similar to OMSs. Among the above natural organic products, sucrose is a competitive carbon source. It is reported that carbon-covered–aluminum could be prepared by the pyrolysis of the dispersed sucrose on alumina [16,17]. The introduction method of carbon was facile and the carbon content was easy to be controlled. In our previous work, we dispersed sucrose on the surface of MCM-48 by the impregnation method [18], and the monolayer dispersion capacity was 1.1 g sucrose/g MCM-48. Herein, we reported the preparation of this new type of sulfonated carbon–silica composites with ordered structure similar to MCM-48. The catalytic performance of the resulting sulfonated carbon–silica composites was examined. The expensive MCM-48 could be easily recycled by simply calcining the composites in air.

2. Experimental

2.1. Preparation of sulfonated carbon–silica composites

MCM-48 was synthesized as follows [19]: 48 g of TEOS (98%) was dissolved in a solution containing 3.8 g of NaOH, 35 g of *n*-hexadecyltrimethylammonium bromide (CTAB) and 200 g of H_2O. The mixture was stirred with magnetic stirring at room temperature for 0.5 h, followed by heating at 373 K in a Teflon-lined autoclave for 3 d. The product was filtered, dried and calcined at 823 K for 6 h in air. Sucrose/MCM-48 composites with different sucrose loadings were prepared by incipient wetness impregnation of 1.0 g of MCM-48 with sucrose aqueous solutions containing 0.8–1.6 g of sucrose, followed by drying at 353 K overnight. After incompletely carbonizing at 673 K in flowing N_2 for 15 h, the white sucrose/MCM-48 composite changed into brown-black carbon/MCM-48. Then, it was heated in a concentrated H_2SO_4 (>96%) solution at 423 K under N_2 for 15 h to introduce $-SO_3H$ into the aromatic carbon rings [7–9]. After cooling it to room temperature, 1000 g of distilled water was added to the mixture to form a black precipitate, which was then washed repeatedly in hot distilled water (>353 K) until sulfate ions were no longer detected in the filtration water by detecting with $BaCl_2$ solution. Sulfonated carbon–silica composites were obtained after drying at 373 K. The final products were denoted MC-0.8, MC-1.0, MC-1.2, MC-1.4 and MC-1.6 when sucrose loadings were 0.8, 1.0, 1.2, 1.4 and 1.6 g, respectively. MC-1.2 before sulfonation was denoted C-MC-1.2.

2.2. Characterization

X-ray diffraction (XRD) was carried out on a Bruker D8 Advance X-ray powder diffractometer with Cu Kα radiation at 40 kV and 30 mA. Morphology analyses were conducted with scanning electron microscopy (SEM, PHILIPS Quanta 200). Transmission electron microscopy (TEM) images were obtained on JEOL JEM 2010 microscope. Elemental analyses were conducted by an energy dispersive X-ray spectrometer (EDX, Genisis) attached to the Quanta 200 microscope. Nitrogen adsorption–desorption isotherms were measured at 77 K using BELSORP II. All samples were degassed at 373 K for 3 h before adsorption measurements. The Brunauer–Emmett–Teller (BET) method was applied to evaluate the total surface area (S_{BET}). The total pore volume was taken from the desorption branch of the isotherm at $P/P_0 = 0.98$ assuming complete pore saturation. The mesoporous volume, pore size distribution and pore diameter were determined from the desorption branch of the isotherm using the Barrett–Joyner–Halenda (BJH) method. X-ray photoelectron spectroscopy (XPS) spectrum was measured using an Axis Ultra spectrometer (Kratos, Manchester, UK) with monochromatic AlKR (1486.71 eV) radiation at a source power of 225 W (15 mA, 15 kV). Acid amounts of the sulfonated carbon–silica composites were estimated by titration with a standard NaOH solution, using a phenolphthalein solution as an indicator.

2.3. Catalytic reactions

The catalytic performance of the sulfonated carbon–silica composites was demonstrated through esterification of acetic acid with n-butyl alcohol (7.4 g of n-butyl alcohol, 3.0 g of acetic acid and 0.10 g of catalyst) at 388 K for 4 h in a 50 ml glass flask equipped with a reflux condenser and a magnetic stirrer under atmospheric pressure. The reaction products were analyzed by a gas chromatog-

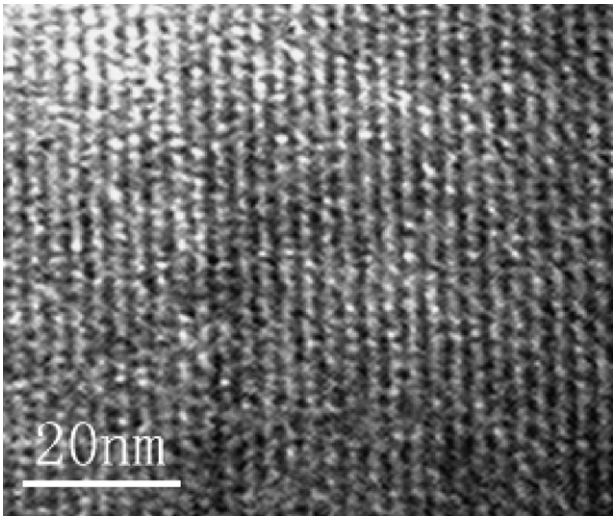

Fig. 2. TEM image of MC-1.2.

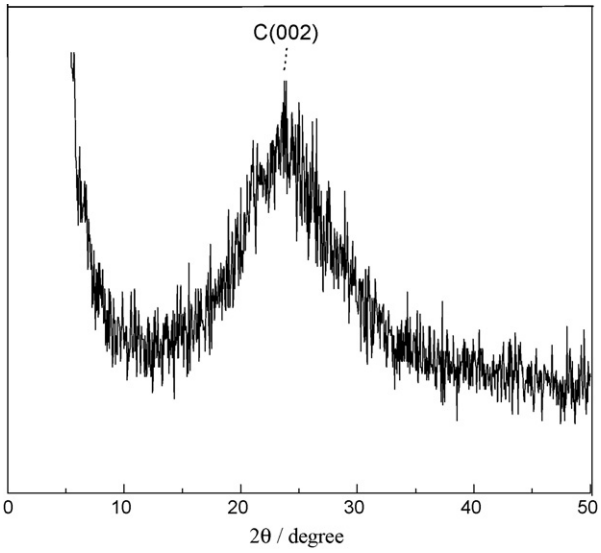

Fig. 3. The wide-angle XRD pattern of MC-1.2.

raphy equipped with an SE-54 capillary column using toluene as an internal standard.

The catalytic activities of the sulfonated carbon–silica composites were also measured in esterification of fatty acids (caprylic acid, lauric acid and hexadecanoic acid) with ethanol at 353 K for 12 h. The reaction solutions were analyzed by titration with a standard NaOH solution to evaluate the yields of the esters. The molar ratio of fatty acid to ethanol was 1:3, and the catalyst amount was 1% of the total reactant mass. Titration was performed for 3 times and the average number was reported.

3. Results and discussion

3.1. Structures of sulfonated carbon–silica composites

In our previous work [18], we found that sucrose could spontaneously disperse on mesoporous MCM-48 molecular sieves to form a monolayer with the monolayer dispersion capacity of sucrose on MCM-48 of about 1.1 g sucrose/g MCM-48. Here we examined the structure of carbon–silica composites, and all of the samples exhibited XRD characteristic peaks at small angles. The sample with a sucrose loading of 1.2 g sucrose/g MCM-48 was taken as an example. Fig. 1 shows small-angle XRD patterns of MCM-48, C-MC-1.2 and MC-1.2. We could see that the XRD pattern of C-MC-1.2 was similar to that of MCM-48, but the peak intensities decreased, which was ascribed to the decrease of scatter contrast between the wall and the pore after dispersion of the carbon [11]. There was no difference in XRD patterns between C-MC-1.2 and MC-1.2, indicating that sulfonation did not result in the structure change of MCM-48 and the carbon. Fig. 2 shows the TEM image of MC-1.2. Parallel strips were observed, which is the same as that of MCM-48 because carbon layer was too thin to be observed [14–20]. These results suggested that dispersion of sucrose, incomplete carbonization and sulfonation did not change the structure of MCM-48. Furthermore, the resulting sulfonated carbon–silica composites still maintained well-ordered mesoporous structures. Fig. 3 shows the wide-angle XRD pattern of MC-1.2. A weak and broad diffraction peak at 2θ of 10–30° (C (0 0 2)) attributed to amorphous carbon composed of aromatic carbon sheets could be obviously observed. A diffraction peak of C (1 0 1) at 2θ of 35–50° was not detected due to the low carbonization temperature applied, indicating that the sample did not form large graphite sheets [9].

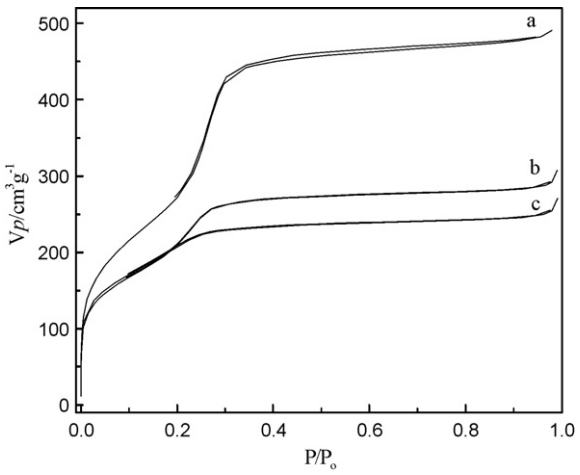

Fig. 4. Nitrogen adsorption–desorption isotherms of MCM-48 (a), MC-0.8 (b) and MC-1.2 (c).

Table 1
Physical properties of MCM-48 and sulfonated carbon–silica composites.

Samples	BET surface area (m^2/g)	Pore volume (cm^3/g)	Mean pore size (nm)	Acid amount of $-SO_3H$ (mmol/g)
MCM-48	998	0.76	2.7	–
MC-0.8	720	0.40	2.2	0.45
MC-1.0	700	0.36	2.1	0.45
MC-1.2	724	0.27	2.0	0.46
MC-1.4	673	0.20	1.7	0.48
MC-1.6	623	0.14	1.5	0.51
CS-sucrose	2	–	–	–
C-MC-1.2	700	0.32	2.0	–

3.2. N_2 adsorption–desorption isotherms

Figs. 4 and 5 show N_2 adsorption–desorption isotherms and corresponding BJH pore size distributions of MCM-48, MC-0.8 and MC-1.2, respectively. Type IV isotherm was observed for MCM-48 [21]. For MC-0.8 and MC-1.2, the total volumes adsorbed were much less than that of MCM-48, and they decreased with the increase of the amount of sucrose loaded. Correspondingly, their isotherms shifted from type IV to type I, suggesting the change of the pore structure from mesopore to micropore range. Table 1 lists BET surface areas, total pore volumes and mean pore sizes of MCM-48, MC-0.8, MC-1.0, MC-1.2, MC-1.4 and MC-1.6. Generally, the total pore volumes and mean pore sizes decreased with the increase of the amount of sucrose loaded. The difference in the pore sizes

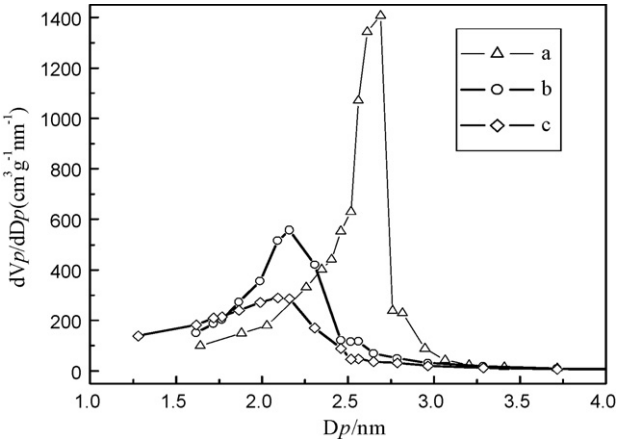

Fig. 5. Pore size distributions of MCM-48 (a), MC-0.8 (b) and MC-1.2 (c).

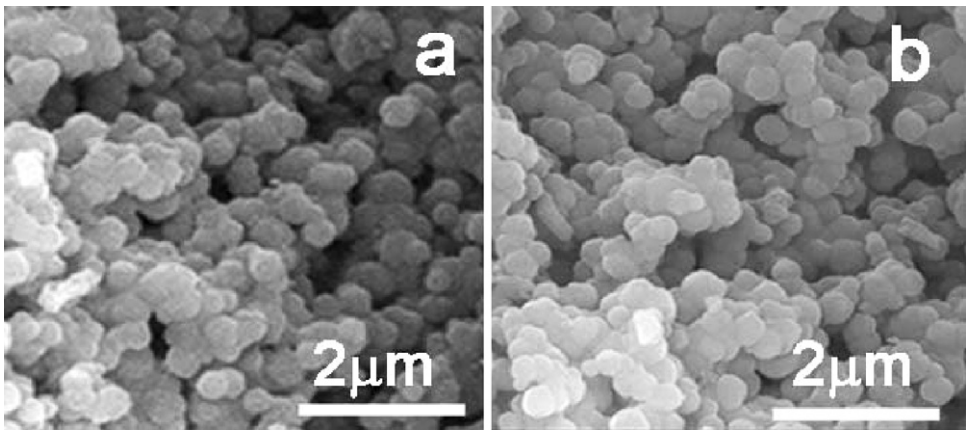

Fig. 6. SEM images of MCM-48 (a) and MC-1.2 (b).

between MCM-48 and MC-1.2 was about 0.7 nm, which was about twice of the thickness of a graphite monolayer, implying that carbon was uniformly deposited on the surface of MCM-48 [17]. BET surface areas were similar for MC-0.8, MC-1.0 and MC-1.2, indicating the formation of carbon monolayer on MCM-48 when the sucrose loadings were close to the monolayer capacity. For MC-1.4 and MC-1.6, their BET surface areas deceased due to the formation of carbon multilayers and nonporous carbon [9–22]. Furthermore, sulfonation did not result in significant change of pore structure and herein the sample before sulfonation (C-MC-1.2) was also listed in Table 1 for comparison. It is noted that pore sizes of the sulfonated composite (1.5–2.2 nm) do not significant differ from that of MCM-48 (2.7 nm), arising from that sucrose tends to disperse on the surface of MCM-48 rather than aggregation [18] and sucrose would remarkably shrink after carbonization.

3.3. Morphology and properties of acid carbon/silica composites

Fig. 6 shows SEM images of MCM-48 and MC-1.2. No obvious differences in morphology were observed. The average particles sizes for both samples were about 500 nm, and these particles were agglomerated. The sulfonated carbon–silica composites showed amphiphilic properties. On one hand, they were insoluble in the solvents (e.g. water, methanol, ethanol, benzene, *N,N*-dimethylformamide, and hexane) even at their boiling temperatures. They could be easily dispersed in these solvents by stirring, and rapidly settled down when stirring stopped. These properties were as same as those of carbon powders produced by incompletely carbonizing D-glucose at temperatures higher than 573 K. On the other hand, the sulfonated carbon–silica composites showed quite good wettability in water, possibly originated from the hydrophilic property of MCM-48.

The sulfonated carbon–silica composites showed quite good hydrothermal stability as their ordered mesoporous structure remained intact after being treated in boiling water for 48 h, as verified from XRD characterization (not shown). For MCM-48, we could not detect any XRD peaks in the small angle range when it was treated in boiling water for 3 h, indicating the collapse of their ordered mesoporous structure. The above results suggested that the hydrothermal stability of the sulfonated carbon–silica composites was greatly enhanced, probably due to the synergism between the carbon and MCM-48.

3.4. Acidity

Fig. 7 shows EDX spectra of C-MC-1.2 and MC-1.2. We could see that C-MC-1.2 contained elements of O and Si derived from MCM-48. MC-1.2 contained another element of S, which was contributed from $-SO_3H$ groups. Fig. 8 shows the XPS spectrum of MC-1.2. Elements of C, O, Si and S were observed, with a single S 2p peak attributed to $-SO_3H$ groups at 168 eV. The acid amounts of sulfonated carbon–silica composites (MC-0.8, MC-1.0, MC-1.2, MC-1.4 and MC-1.6) were in the range of 0.45–0.51 mmol/g (Table 1), which were less than those of sulfonated carbon composites reported in the literature [10] as silica contributed much to the weight of the composites. For example, carbon accounts for 27.0 wt% in MC-1.2. Thus, the acid amount of MC-1.2 based on the weight of carbon was as high as 1.6 mmol/g.

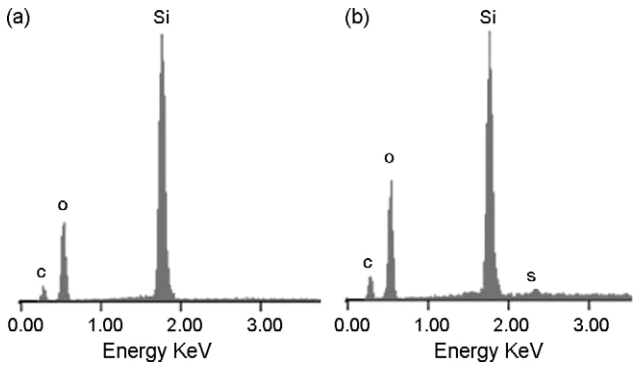

Fig. 7. EDX spectra of C-MC-1.2 (a) and MC-1.2 (b).

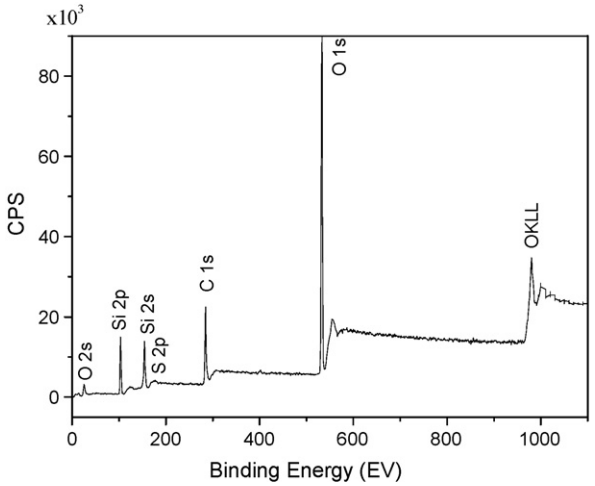

Fig. 8. XPS spectrum of MC-1.2.

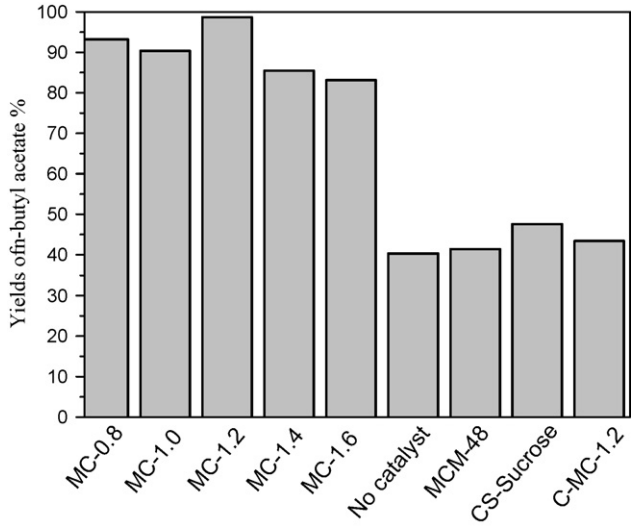

Fig. 9. Catalytic activities of various catalysts in the esterification of acetic acid with n-butyl alcohol.

3.5. Catalytic performance

Fig. 9 shows the histogram of yields of n-butyl acetate catalyzed by sulfonated carbon–silica composites. For comparison, C-MC-1.2, MCM-48, and incompletely carbonized and sulfonated sucrose (denoted as CS-sucrose) were also applied as the catalysts in the production of n-butyl acetate. We could see that the yield of butyl acetate was 40.3% at 388 K for 4 h without a catalyst, and the yield almost did not change when MCM-48 and C-MC-1.2 were used as catalysts, indicating that MCM-48 and C-MC-1.2 have low catalytic activities in this reaction. CS-sucrose exhibited a little high catalytic activity with a n-butyl acetate yield of 47.5% because the presence of the $-SO_3H$ groups. On the other hand, sulfonated carbon–silica composites exhibited obvious high activities in the esterification of n-butyl alcohol with acetic acid. The yields of n-butyl acetate on MC-0.8, MC-1.0 and MC-1.2 reached 93.2%, 90.4%, and 98.7%, respectively, which were almost twice higher than those on MCM-48, C-MC-1.2 and CS-sucrose. MC-1.4 and MC-1.6 had relatively low catalytic activities and the corresponding yields of n-butyl acetate were 85.5% and 83.1%, respectively. The activities of sulfonated carbon–silica composites prepared under optimized condition were comparable with the solid acids reported in Refs. [23,24]. It is worth mentioning that MC-1.2 prepared with the used MCM-48 exhibited a n-butyl acetate yield of 96.5% under the same reaction condition, suggesting that expensive sulfonated carbon–silica composites could be recycled.

The correlation of the catalytic activity and $-SO_3H$ density as well as pore parameters was also studied (Table 1 and Fig. 9). For the samples with similar surface area, MC-1.2 with more acid amount exhibited higher activity than MC-0.8. While MC-1.4 and MC-1.6 with higher $-SO_3H$ density but lower surface area exhibited lower activity than MC-1.2. This is because both high acid density and high surface area favor the catalytic reaction.

As MC-1.2 showed the highest catalytic activity in the esterification of acetic acid with n-butyl alcohol, it was thus examined in the esterification of long-chain fatty acids with ethanol. Table 2 shows yields of ethyl caprylate, ethyl laurate and ethyl hexadecanoate with and without a catalyst. It could be seen that the yields of long-chain fatty acid esters were much higher on MC-1.2 than that without a catalyst, referring the apparent catalytic activity of MC-1.2. On the other hand, CS-sucrose was also used as the catalyst in these esterification reactions. However, it exhibited yields of the long-chain fatty acid esters almost similar to those without a catalyst, obviously due to the nonporous structure of CS-sucrose.

Table 2
Yields of ethyl caprylate, ethyl laurate and ethyl hexadecanoate with and without a catalyst.

Reaction	Yields (%)	
	No catalyst	MC-1.2
Caprylic acid + ethanol	29	48
Lauric acid + ethanol	18	58
Hexadecanoic acid + ethanol	23	56

4. Conclusions

Sulfonated carbon–silica composites with ordered pore structure and high surface areas (>600 m^2/g) were prepared by sulfonation of incompletely carbonized sucrose on MCM-48. Carbonization and sulfonation did not change the well-ordered structure of MCM-48. By controlling the loading of sucrose on MCM-48, the surface area, pore sizes and the catalytic activities of the resulting sulfonated carbon–silica composites could be adjusted. The composites exhibited enhanced hydrothermal stability and amphiphilic property. The yields of n-butyl acetate were higher than 83.1% in the esterification of acetic acid with n-butyl alcohol. The mesoporous sulfonated silica–carbon composites were accessible for long-chain fatty acids and exhibited obvious catalytic activities in the esterification of long-chain fatty acids with ethanol.

Acknowledgments

This work was supported by the Shanghai Key Laboratory of Green Chemistry and Chemical Processes at East China Normal University.

References

[1] J.H. Clark, Acc. Chem. Res. 35 (2002) 791–797.
[2] D. Margolese, J.A. Melero, S.C. Christiansen, B.F. Chmelka, G.D. Stucky, Chem. Mater. 12 (2000) 2448–2459.
[3] J.G.C. Shen, R.G. Herman, K. Klier, J. Phys. Chem. B 106 (2002) 9975–9978.
[4] V. Dufaud, M.E. Davis, J. Am. Chem. Soc. 125 (2003) 9403–9413.
[5] J. Chen, M. Han, R. Sun, J.T. Wang, Chin. J. Inorg. Chem. 22 (2006) 1568–1572.
[6] M. Hara, T. Yoshida, A. Takagaki, T. Takata, J.N. Kondo, S. Hayashi, K. Domen, Angew. Chem. Int. Ed. 43 (2004) 2955–2958.
[7] M. Toda, A. Takagaki, M. Okamura, J.N. Kondo, S. Hayashi, K. Domen, M. Hara, Nature 438 (2005) 178.
[8] V. Budarin, J.H. Clark, J.J.E. Hardy, R. Luque, K. Milkowski, S.J. Tavener, A.J. Wilson, Angew. Chem. Int. Ed. 45 (2006) 3782–3786.
[9] M. Okamura, A. Takagaki, M. Toda, J.N. Kondo, K. Domen, T. Tatsumi, M. Hara, S. Hayashi, Chem. Mater. 18 (2006) 3039–3045.
[10] R. Xing, Y.M. Liu, Y. Wang, L. Chen, W.H. Wu, Y.W. Jiang, M.Y. He, P. Wu, Micropor. Mesopor. Mater. 105 (2007) 41–48.
[11] X.Q. Wang, R. Liu, M.M. Waje, Z.W. Chen, Y.S. Yan, K.N. Bozhilov, P.Y. Feng, Chem. Mater. 19 (2007) 2395–2397.
[12] M.M.L. Ribeiro Carrott, A.J.E. Candeias, P.J.M. Carrott, K.S.W. Sing, K.K. Unger, Langmuir 16 (2000) 9103–9105.
[13] S.S. Kim, K.D. Lee, J. Shah, T.J. Pinnavaia, Chem. Commun. (2003) 1436–1437.
[14] S.M. Zhu, H.S. Zhou, M. Hibino, I. Honma, M. Ichihara, Mater. Chem. Phys. 88 (2004) 202–206.
[15] H. Nishihara, Y. Fukura, K. Inde, K. Tsuji, M. Takeuchi, T. Kyotani, Carbon 46 (2008) 48–53.
[16] Y.X. Zhu, X.M. Pan, Y.C. Xie, Acta Phys. Chim. Sinica 15 (1999) 830–833.
[17] L. Lin, W. Lin, Y.X. Zhu, B.Y. Zhao, Y.C. Xie, G.Q. Jia, C. Li, Langmuir 21 (2005) 5040–5046.
[18] J. Chen, C.F. Zeng, L.X. Zhang, N.P. Xu, Acta Phys. Chim. Sinica 23 (2007) 1463–1467.

[19] R. Ryoo, S.H. Joo, S. Jun, J. Phys. Chem. B 103 (1999) 7743–7746.
[20] K. Schumacher, P.I. Ravikovitch, A.D. Chesne, A.V. Neimark, K.K. Unger, Langmuir 16 (2000) 4648–4654.
[21] Y.F. Shao, L.Z. Wang, J.L. Zhang, M. Anpo, Micropor. Mesopor. Mater. 86 (2005) 314–322.
[22] X.H. Mo, D.E. Lopez, K. Suwannakarn, Y.J. Liu, E. Lotero, J.G. Goodwin Jr., C.Q. Lu, J. Catal. 254 (2008) 332–338.
[23] N. Bhatt, A. Patel, P. Selvam, K. Sidhpuria, J. Mol. Catal. A 275 (2007) 14–24.
[24] V.S. Braga, I.C.L. Barros, F.A.C. Garcia, S.C.L. Dias, J.A. Dias, Catal. Today 133–135 (2008) 106–112.